

REPORT DOCUMENTATION PAGE			Form Approved OMB No. 0704-0188	
Public reporting burden for this collection of information is estimated to average 1 hour per response, including the time for reviewing instructions, searching existing data sources, gathering and maintaining the data needed, and completing and reviewing the collection of information. Send comments regarding this burden estimate or any other aspect of this collection of information, including suggestions for reducing this burden to Washington Headquarters Services, Directorate for Information Operations and Reports, 1215 Jefferson Davis Highway, Suite 1204, Arlington, VA 22202-4302, and to the Office of Management and Budget, Paperwork Reduction Project (0704-0188), Washington, DC 20503.				
1. AGENCY USE ONLY (Leave blank)	2. REPORT DATE 10/10/98	3. REPORT TYPE AND DATES COVERED Final, 12/01/94 to 06/30/97		
4. TITLE AND SUBTITLE Time-Resolved Picosecond Spectroscopy in Shock Wave Experiments: Experimental Developments		5. FUNDING NUMBERS G N000149510311		
6. AUTHOR(S) Y.M. Gupta (Principal Investigator) Contributors: M.D. Knudson and K.A. Zimmerman				
7. PERFORMING ORGANIZATION NAMES(S) AND ADDRESS(ES) Institute for Shock Physics and Department of Physics Washington State University PO Box 642816 Pullman, Washington 99164-2816		8. PERFORMING ORGANIZATION REPORT NUMBER OGRD 41788		
9. SPONSORING / MONITORING AGENCY NAMES(S) AND ADDRESS(ES) Office of Naval Research Code 1132P 800 N. Quincy St. Arlington, Virginia 22217		10. SPONSORING / MONITORING AGENCY REPORT NUMBER 200-250		
11. SUPPLEMENTARY NOTES This report has been submitted to the Rev. Sci. Instruments for publication.				
a. DISTRIBUTION / AVAILABILITY STATEMENT Unlimited Distribution		12. DISTRIBUTION CODE		
13. ABSTRACT (Maximum 200 words) An experimental method was developed to perform picosecond time-resolved electronic spectroscopy in single-event, plate impact, shock wave experiments. Several experimental difficulties had to be addressed due to the fast time resolution (100 ps) and short time duration (12.7 ns) of such experiments. Procedures are described to address the following experimental issues: (i) synchronization of the light source, detection equipment, and the shock event within the experimental duration, (ii) incorporation of a Nd:YAG laser (operative in a repetitive mode) into the experimental configuration, and (iii) sources of temporal dispersion. Representative results are shown from experiments performed on single crystal CdS. The developments described here are also expected to be useful for shock wave experiments involving Raman, fluorescence, or other types of spectroscopy which require the use of a laser.				
14. SUBJECT TERMS Shock waves, optical spectroscopy, picosecond, structural changes			15. NUMBER OF PAGES 24	
			16. PRICE CODE	
17. SECURITY CLASSIFICATION OF REPORT Unclassified	18. SECURITY CLASSIFICATION OF THIS PAGE Unclassified	19. SECURITY CLASSIFICATION OF ABSTRACT Unclassified	20. LIMITATION OF ABSTRACT UL	

Standard Form 298 (Rev. 2-89)  
Prescribed by ANSI Std Z39-18  
298-102

# Picosecond Time-Resolved Electronic Spectroscopy in Plate Impact Shock Experiments: Experimental Development

M.D. Knudson, K.A. Zimmerman, and Y.M. Gupta

Institute for Shock Physics and Department of Physics, Washington State University, Pullman,  
WA 99164-2816

## ABSTRACT

An experimental method was developed to perform picosecond time-resolved electronic spectroscopy in single-event, plate impact, shock wave experiments. Several experimental difficulties had to be addressed due to the fast time resolution (100 ps) and short time duration (12.7 ns) of such experiments. Procedures are described to address the following experimental issues: (i) synchronization of the light source, detection equipment, and the shock event within the experimental duration, (ii) incorporation of a Nd:YAG laser (operative in a repetitive mode) into the experimental configuration, and (iii) sources of temporal dispersion. Representative results are shown from experiments performed on single crystal CdS. The developments described here are also expected to be useful for shock wave experiments involving Raman, fluorescence, or other types of spectroscopy which require the use of a laser.

19981204 018

## I. Introduction

Under extreme pressure and temperature conditions condensed materials can undergo a variety of time-dependent phenomena, including chemical reactions<sup>1,2</sup> and phase transformations.<sup>3,4</sup> Plane shock wave experiments provide a method which is well suited to investigate the dynamic response of condensed materials to these extreme conditions.<sup>5</sup> The very rapid and macroscopically well defined loading conditions in these experiments permit real-time examination of shock-induced chemical reactions and phase transformations. Such studies have generally been performed at the continuum level for several decades.<sup>6-11</sup> However, despite these efforts, detailed understanding of the atomic and molecular mechanisms governing these processes is lacking. One notable exception is the recent work of Gruzdkov and Gupta<sup>12,13</sup> in determining the molecular mechanisms governing the shock-induced decomposition of amine sensitized nitromethane.

The lack of mechanistic understanding is primarily due to the lack of experimental data at the atomic/molecular level. Typical methods used to obtain data at the atomic/molecular level in condensed materials, e.g. x-ray diffraction and optical spectroscopies such as absorption, emission, Raman, etc., are difficult to incorporate into shock wave experiments, due to the complexity of such measurements.<sup>5</sup> These measurements are further complicated by the high rates likely associated with shock-induced chemical changes and phase transformations. For example, a phase transformation rate of  $5 \times 10^8 \text{ sec}^{-1}$  was inferred for single crystal potassium chloride shocked to sufficiently high stress.<sup>14</sup> Thus, to resolve the atomic/molecular changes under shock loading, fast time resolution measurements are needed.

Over the past two decades, methods have been developed to perform ns time-resolved optical spectroscopies in plate impact shock experiments; these include absorption,<sup>12,15-18</sup> reflection,<sup>19</sup> fluorescence,<sup>13</sup> and Raman.<sup>20-24</sup> Measurements with this time resolution are well suited to probe the atomic/molecular changes associated with shock-induced chemical reactions; 50 ns time-resolved absorption and fluorescence measurements were used by Gruzdkov and Gupta<sup>12,13</sup> in their work on sensitized nitromethane. However, the time scales involved in shock-induced phase transformations are typically much shorter.<sup>10</sup> Thus, the ability to obtain real-time

information, with sub-nanosecond resolution at the atomic/molecular level, is an important need for identifying the mechanisms governing pressure-induced phase transformations, and for understanding the high rates of transformation associated with many shock-induced transitions. Addressing this need was the motivation for this work.

In this article, we report on the development of an experimental method to perform picosecond time-resolved electronic spectroscopy in plate impact experiments. The method builds upon previous work used to obtain nanosecond time-resolved measurements.<sup>12,15-18</sup> However, due to the faster time resolution (100 ps) and the considerably shorter time duration (12.7 ns) of these experiments, several issues not relevant on the nanosecond time scale become important at the picosecond time scale. In the next section an overview of the experimental configuration is presented. Section III provides a detailed discussion of the experimental considerations, emphasizing the important issues on the picosecond time scale. Particular attention is given to the methods developed to overcome the synchronization difficulties, and to the two different approaches used to incorporate a Nd:YAG laser in single-event, plate impact experiments. Representative results are shown in section IV, and concluding remarks are given in section V.

## II. Experimental Configuration

The experimental configuration used to achieve 100 ps time resolution in single-event impact experiments is shown in Fig. 1. Shock waves were generated by the planar impact of a transparent impactor (sapphire,  $\alpha$ -quartz, or fused silica), mounted on a projectile accelerated by a single-stage light gas gun,<sup>25</sup> onto the target assembly. The latter consisted of two optically transparent buffer windows (sapphire or  $\alpha$ -quartz) backed by the sample. Three piezoelectric trigger pins (Dynasen, Inc., CA-1135), located concentrically around the probed region of the sample, were placed behind the front buffer window to provide both a trigger pulse from the shock front and a timing fiducial for the arrival of the shock wave at the interface between the front and mid buffer windows. The second buffer window provided a traversal delay to offset the insertion delays of the experimental components, enabling synchronization of the light source, detection equipment, and the arrival of the shock wave at the sample.

Fluorescence from a Nd:YAG (Continuum, custom built laser) pumped dye solution, consisting of a mixture of Coumarine 500 and DCM laser dyes, was used as the light source for the experiments. The resulting 12 ns FWHM fluorescence pulse covered the wavelength spectrum from about 500 to 700 nm. Two flat mirrors, located on the projectile, directed the light through the sample where it was collected into a fiber bundle, consisting of two 200  $\mu\text{m}$  core optical fibers. This arrangement provided single pass absorption/transmission through the sample. One fiber directed the signal to a fast photodiode (Thorlabs, Inc., DET2-SI), which was used as a timing diagnostic. The second fiber delivered the transmitted signal to the picosecond detection system. The signal was first spectrally dispersed by a spectrometer (SPEX 500M, 150 gr/mm grating). The spectrally dispersed output of the spectrometer was then incident on a fast streak camera (Hadland Photonics, Imacon 500), which temporally dispersed the signal. The output of the streak camera, a two-dimensional distribution of light intensity with wavelength along one axis and time along the other, was intensified with a micro-channel plate (MCP) image intensifier (Photek, MCP140), and digitally recorded on a CCD detector (Princeton Instruments, LN/CCD-1024 TKB/1). The CCD image was binned along the time axis into 127 spectra, each separated in time by 100 ps.

As this method utilizes a streak camera to temporally disperse the optical signal, a streak camera capable of fast enough streak rates would, in principle, enable one to perform picosecond time resolution experiments using an experimental configuration identical to that used for nanosecond measurements. However, an increase in the streak rate of the camera results in a corresponding decrease in the total recording time of the experiment. In the present case, increasing the time resolution from 50 ns to 100 ps resulted in a decrease in the total time duration of the experiments from 2.55  $\mu\text{s}$  to 12.7 ns. Due to the increased time resolution and the very short time duration of these experiments, several issues become important. These issues include (i) the synchronization of the light source, detection equipment, and the shock event within the 12.7 ns experimental duration, (ii) the incorporation of a Nd:YAG laser, used to provide sufficient light intensity to perform the absorption/transmission measurement, into the experimental configuration, and (iii) sources of temporal dispersion. The next section discusses each of these issues and describes how they were addressed in the present experimental configuration.

### III. Experimental Considerations

#### A. Synchronization

In nanosecond experiments, the trigger signal is obtained by the shorting of a trigger pin by the projectile face prior to impact.<sup>12,15-18</sup> This arrangement can result in relatively large uncertainties in synchronization of the experimental components with the impact event; uncertainty in the projectile velocity (in gas gun experiments, projectile velocities can only be predicted to within a few percent) leads to uncertainties in the time of flight prior to impact. Even for trigger pins at the impact surface, the uncertainty in the height of the impactor from the projectile face and the position of the pin relative to the target face are large enough to preclude this approach. Since shock wave velocities are unchanged by small variations in projectile velocities, a consistent and reliable method of triggering from the shock front can be used to avoid the uncertainty introduced by triggering from the projectile.

Piezoelectric trigger pins were chosen to provide a trigger pulse from the shock front. The pins were 0.064" diameter by 1" long coaxial probes which contain a small 1 mm diameter by 0.5 mm thick PZT-5A crystal. The typical voltage pulse obtained from these pins, when shock compressed, has a pulse width of roughly 100 ns and a peak voltage of about 120 V. Provided that the surface of the pin is parallel to the shock front, the rise time of the voltage pulse is on the order of 2 to 4 ns.<sup>26</sup> To condition the trigger signal, the output of the piezoelectric pin was delivered to a fast rise time pulse generator. The pulse generator output, roughly 1  $\mu$ s in duration with a peak voltage of 100 V, was used to trigger the experimental components. The insertion delay and jitter of the pulse generator was approximately 16 ns and less than 0.5 ns, respectively.

Triggering from the shock front reduces one source of timing uncertainty; however, a second source of uncertainty is caused by non-planar impact, or tilt. Measures can be taken to minimize the magnitude of the tilt (improved projectile design, target alignment, etc.) but tilt cannot be eliminated. Non-planar impact results in a line of contact sweeping across the target face with a velocity that depends upon the projectile velocity and the tilt:

$$v_{\text{contact}} = \frac{v_{\text{proj.}}}{\tan \theta} \quad (1)$$

where  $\theta$  is the angle between the impactor and the target surface. Using typical values for  $v_{\text{proj.}}$  and  $\theta$  (0.5 to 0.6 mm/ $\mu$ s and 0.3 to 0.8 mrad, respectively),  $v_{\text{contact}}$  ranged from 0.63 to 2 mm/ns.

As discussed below, these values are significant for the time scales involved in picosecond measurements. They are large enough to make synchronization difficult, and alter the effective time resolution.

Since these measurements involve optical transmission, the probed region and the trigger pin position must be separated laterally (see Fig. 1). The smallest distance feasible between the probed region and the trigger pin in these experiments was approximately 7 mm. Thus, the time difference due to tilt between impact of the target surface directly above the trigger pin and directly above the probed region is on the order of 3 to 12 ns. Considering that the total time duration of the experiment is 12.7 ns, this uncertainty of  $\pm 12$  ns is quite significant. In fact, the synchronization difficulty due to non-planar impact limited the time resolution of the present experiments.

The approach used to reduce this uncertainty involved placing three pins concentrically around the probed region, as shown in Fig. 1. The signals from these pins were combined using high-voltage, fast recovery diode isolators (Newark Electronics, P/N 1P648), thus the first pin to be shocked provided the trigger pulse for the pulse generator. The use of three concentric pins around the probed region ensured that the target surface above one of the three pins would be impacted prior to the surface above the probed region. Thus, the uncertainty was reduced by a factor of two, with the time difference between impact of the surface above a pin and the probed region ranging from + 0 to - 12 ns.

To further reduce the uncertainty in knowing the arrival time of the shock wave at the probed region, a particular magnitude of tilt was assumed and its effect incorporated into the experimental timing. The typical value of tilt observed was 0.5 mrad; thus the effect of a 0.5 mrad tilt was incorporated. For example, if the desired projectile velocity was 0.6 mm/ $\mu$ s, the expected time difference between impact of the target surface above a pin and the probed region was 5.8 ns. This delay due to tilt was then added to the traversal delay of the shock wave through the mid buffer window to determine the time at which the shock event was expected to occur. This time was compared to the propagation delay of the trigger signals through the various cables and the insertion delays of the experimental components. A cable delay box (EG&G Ortec, model DB463) was then used to provide the necessary delays in the trigger signals to ensure synchronization of the various experimental components with the shock event. The actual tilts observed in these experiments ranged from 0.3 to 0.8 mrad, resulting in time differences of 3.5 to



9.3 ns. With this procedure, the uncertainty in knowing the arrival of the shock wave at the sample ranged from 2 to 4 ns.

## **B. Incorporation of the Nd:YAG Laser**

The time scales associated with the picosecond absorption/transmission experiments require the use of a relatively high intensity light source. The light source used to perform the absorption/transmission measurements was the fluorescence from a Nd:YAG pumped dye solution, consisting of Coumarine 500 and DCM laser dyes. However, Nd:YAG lasers are temperature sensitive and are designed to operate at the relatively constant elevated temperatures achieved while running in repetitive mode.<sup>27</sup> Thus, the initial pulses of the laser upon start up are unstable. Further, unless the Nd:YAG laser is seeded, the temporal output of the pulse will show significant intensity modulation over the pulse length due to mode beating effects.<sup>27</sup> By seeding the laser output, this mode beating is eliminated. However, for optimal seeding, the frequency of the diode seed laser must match the Nd:YAG laser cavity mode frequency. Thus the laser must be running at some repetitive rate so that the seeding performance can be monitored and adjusted accordingly. For these reasons, it is not feasible to use a Nd:YAG laser in single shot mode; thus, the incorporation of a Nd:YAG laser into single-event, plate impact experiments is not straightforward.

The important issue in incorporating the Nd:YAG laser in single-event, plate impact experiments is how to correlate the shock event with the repetitive firing of the laser. Two different approaches were used and are described below. Further details concerning the stability issues of the seeded Nd:YAG laser, including the sensitivity of the laser performance on such factors as (i) the time interval between the firing of the flashlamp and the firing of the q-switch, and (ii) the difference in the time interval between the laser pulse obtained during the shock experiment and the pulse immediately prior to the experiment with the fixed time interval defined by the repetition rate of the laser, can be found elsewhere.<sup>28</sup>

In the initial picosecond experiments, the method used to correlate the shock event with the repetitive firing of the laser was to synchronize the Nd:YAG laser to the firing of the gas gun. Fig. 2 shows a schematic view of the electrical configuration used. Three trigger pulses were required for the laser: a pulse to initiate the charging of the capacitors in the flashlamp power supply, a pulse to trigger the flashlamps, and a pulse to trigger the q-switch. These pulses were



supplied by a digital delay generator (Stanford Research Systems, Inc., model D6535) set at a repetition rate of 1.5 Hz. Two of these pulses, the flashlamp and q-switch trigger pulses, were routed through a switch which was connected to the fire button on the control panel of the gun. Upon pressing the fire button, these signals were interrupted and the laser ceased firing in a repetitive mode, but the capacitors still received the charge pulse. The flashlamp and q-switch trigger pulses for the shock experiment were then initiated by the contact of a set of shorting wires in the barrel of the gun by the projectile, and the trigger pulse obtained from the piezoelectric trigger pins, respectively. Appropriate delays in these trigger pulses were obtained from additional delay generators.

Although this method of synchronization worked, there were some undesirable consequences. To avoid instability due to thermal effects caused by the variation in the time between successive pulses, the laser was set to run at a repetition rate of 1.5 Hz.<sup>28</sup> However, the operation of the laser at a repetition rate of 1.5 Hz was too low to enable the use of the auto-seed feature of the seeder controller; the frequency of sampling the build up time is too low, and the seeder begins to simply scan the position of the end mirror in an attempt to bring the laser into seed. Thus the seeder controller had to be set to operate in the manual mode.<sup>27</sup> However, in comparison to the auto-seed mode, this method of seeding is relatively unstable. Further, this method required the output pulse of the laser to be continually monitored by the experimenter, which further complicated the experiment.

This method of synchronization also resulted in large deviations in the time interval between the laser pulse obtained during the shock experiment and the pulse obtained immediately prior to that pulse. At a rate of 1.5 Hz, the laser fires at regular intervals of 667 ms. It was discovered during the course of this study that the time between the pressing of the fire button and impact of the projectile at the target was consistently  $230 \pm 20$  ms. Thus, as seen in the timelines shown in Fig. 3, the time difference between the laser pulse obtained during the experiment and the pulse immediately prior could vary between 210 to 910 ms. Eventhough the thermal instability effects are reduced by running the laser at 1.5 Hz, as seen in Fig. 4, this jitter in the time difference between pulses was enough to cause relatively significant changes in the build up time of the laser pulse obtained in the shock experiment, particularly when the time difference was less than approximately 400 ms.<sup>28</sup>

For the later picosecond experiments, an improvement was made in the method described above to correlate the shock event with the repetitive firing of the laser. The electrical configuration was almost identical to that shown in Fig. 2, with the exception being in the switch at the control panel of the gun. After analyzing the diagnostics from several experiments it was discovered that the time between the firing of the gun and impact of the projectile at the target was consistently  $230 \pm 20$  ms. This regularity in the firing of the gun made it possible to alter the method of synchronization such that the gun was synchronized to the Nd:YAG laser which was set to run at a repetition rate of 5 Hz. To do this, a logic circuit was constructed to replace the analog switch at the gun control panel.<sup>29</sup>

The logic switch worked as follows (refer to the timeline shown in Fig. 5). After the fire button was pressed the circuit waited for the next charge pulse from the pulse generator. This synchronized the logic circuit to the laser. Once the circuit received the charge pulse it waited an additional 100 ms before opening the valves in the breech, thus firing the gun, and allowed the pulse generator to fire the laser one more time before interrupting the flashlamp and q-switch trigger pulses. The flashlamp and q-switch trigger pulses for the next laser pulse, which corresponded to the shock experiment, were initiated by the barrel short and the piezoelectric trigger pins, respectively.

This method of synchronizing the gun to the laser avoided the problems exhibited when synchronizing the laser to the gun. The repetition rate of 5 Hz was high enough that the auto-seed feature of the seeder could be employed. Also, the jitter in the time difference between the laser pulse obtained in the shock experiment and the pulse immediately prior was  $\pm 20$  ms, which corresponds to the jitter in the time between the firing of the gun and impact. This reduction in the jitter, from  $+240/-460$  ms to  $\pm 20$  ms, greatly improved the stability of the laser pulse.

### C. Temporal Dispersion

Due to the very short time scales associated with picosecond experiments, sources of temporal dispersion need to be examined carefully. One source of temporal dispersion is due to non-planar impact, or tilt, and the finite spot size at the sample through which light is transmitted into the optical fiber; the spot size depends upon the core size of the optical fiber. The signal collected into the optical fiber is dispersed temporally by the time required for the line of contact to sweep across (Eq. 1) the collection spot. To reduce the effect of temporal dispersion due to

non-planar impact, while maintaining sufficient signal strength for the absorption/ transmission measurement, a 200  $\mu\text{m}$  core collection fiber was used in the experiments. Thus, typical dispersion due to tilt in these experiments ranged from 100 to 320 ps. The actual dispersion for each experiment differed, depending on the tilt and projectile velocity for the particular experiments.

There are two additional sources of temporal dispersion introduced by the propagation of light through an optical fiber: modal dispersion and chromatic dispersion.<sup>30</sup> Modal dispersion, which occurs in large core multimode fibers, increases as the acceptance angle of the fiber increases. To decrease the effect of temporal dispersion due to modal dispersion, an f/4 optical fiber (relatively small acceptance angle of approximately  $7^\circ$ ) was used to deliver the collected signal to the detection system. The modal dispersion of this fiber is approximately 17.7 ps/meter.<sup>30</sup> Roughly 15 meters of optical fiber was used to deliver the signal to the detection system; thus the total modal dispersion through the fiber was approximately 270 ps. However, this analysis assumes that an axial ray remains on axis throughout the length of the fiber. Bends in the fiber introduce modal mixing and reduces the actual dispersion through the fiber.<sup>30</sup>

Chromatic dispersion is due to the wavelength dependence of the index of refraction and results in the wavelength dependence of the propagation speed through the fiber. A fused silica core fiber was used in these experiments to transmit light in the spectral range of 500 to 700 nm. The index of refraction of fused silica at 500 and 700 nm is  $n = 1.462$  and  $n = 1.455$ , respectively.<sup>31</sup> This difference in the index of refraction results in a difference in traversal time of approximately 22.4 ps per meter of optical fiber; the chromatic dispersion through the length of the fiber was approximately 340 ps. However, since the signal is dispersed in wavelength at the detection system, chromatic dispersion is not as significant an issue as modal dispersion and dispersion due to tilt. Chromatic dispersion merely resulted in the appearance of shock induced changes in the absorption/transmission at the detector at slightly later times for the shorter wavelengths. This effect was observed in the experimental data and was accounted for.

Finally, in shock wave experiments spatial and temporal resolution are linked by the velocity of the shock wave through the material of interest. In picosecond experiments this relation between spatial and temporal resolution becomes important. A typical shock velocity in a solid is on the order of 5 mm/ $\mu\text{s}$ , or expressed in more appropriate units, 5  $\mu\text{m}/\text{ns}$ . To truly realize 100 ps time resolution, either the collected signal must come from a very thin region of

the sample or the thickness of the sample itself must be on the order of 0.5  $\mu\text{m}$  or less. In the current study, the very different nature of the electronic structure of the ambient and high pressure phases of CdS allowed for fast time resolution measurements, even in relatively thick crystals. The ambient pressure phase of CdS exhibits a direct band gap with an energy gap of about 2.5 eV,<sup>32</sup> while the high pressure rocksalt phase is found to be an indirect band gap semiconductor with an energy gap of about 1.5 eV.<sup>33,34</sup> Therefore, there is a wide wavelength range between 500 and 800 nm which is essentially transparent to the ambient phase but is highly absorbing in the high pressure phase. Thus, measurements of the absorption/transmission in this wavelength range probed only the material behind the shock front.

Considering all sources of temporal dispersion, the actual time resolution achieved in the present experiments was approximately 200 to 300 ps. The primary source of dispersion in these experiments was modal dispersion, due to a relatively long fiber length necessary to direct the collected signal from the experimental chamber to the detection system. To reduce the effect of modal dispersion, either shorter lengths of fibers could be used (requiring the detection equipment to be located in close proximity of the experimental chamber) or the signal could be directly coupled to the detection equipment.

#### IV. Representative Results

As representative data obtained using the experimental configuration described above, we show the results of an experiment performed on single crystal CdS reported previously.<sup>35</sup> The crystal was shocked along the *c*-axis to a stress of approximately 8.8 GPa, determined from the known shock response of CdS and the buffer materials<sup>36-38</sup> and the measured projectile velocity. This stress value was well above the phase transition threshold stress of 3.3 GPa reported by Tang and Gupta.<sup>36</sup> Fig. 6 displays the integrated intensity of light transmitted through the sample, obtained from the photodiode diagnostic, for both the shock experiment and a reference pulse taken just prior to the shock experiment. The arrival of the shock front at the CdS sample is indicated in the figure by a dotted line. Immediately following the arrival of the shock front there occurred a dramatic decrease in transmission. The arrival time was determined from a tilt analysis of the three trigger pin records, which indicated the arrival of the shock wave at the front and mid buffer interface directly above the probed region of the sample, and the calculated

traversal time through the mid buffer window. The uncertainty in the timing, due to uncertainty in both the tilt analysis and the wave speed of the buffer material, was on the order of 1 to 2 ns. Also indicated in the figure, by dashed lines, are the beginning and the end of the streak record for this particular experiment. This figure illustrates the synchronization needs due to the very short time-duration of the streak record and the light pulse.

Time-resolved, spectral information was obtained from the picosecond detection system. Fig. 7a displays the results as a plot of absorbance versus wavelength and time. Absorbance values were determined by comparing the intensities of the streak record obtained during the shock experiment with a reference streak using the expression

$$\text{Absorbance} = -\ln \frac{I}{I_0}, \quad (2)$$

where  $I$  and  $I_0$  are the intensities obtained from the shock experiment and the reference streak, respectively. In accordance with the photodiode results, once the shock front reached the CdS sample, indicated by  $t = 0$  in the streak record, the absorbance increased dramatically. The time dependence of the absorbance behind the shock front can be seen most easily in Fig. 7b, which displays absorbance versus time for several different wavelengths. As seen in the figure, the absorbance at a given wavelength increased linearly with time, with a slope which increased with decreasing wavelength. The linear increase in absorbance with time reflects the propagation of the shock front through the sample; as the shock front propagated through the CdS sample, more material was subject to uniaxial strain. Thus the linear time dependence suggests that behind the shock front the absorption coefficient, though wavelength dependent, was time independent, at least for this experiment.

Using a value of  $4.3 \text{ mm}/\mu\text{s}$  for the shock wave velocity through the CdS sample, taken from the study performed by Tang and Gupta,<sup>36</sup> the slope of the absorbance increase was used to determine the absorption coefficient for the material behind the shock front. For a given wavelength the absorbance data corresponding to  $t > 0$  were fitted to a linear function. The slope was then divided by the shock wave velocity to obtain the absorption coefficient. The resulting absorption coefficient as a function of wavelength is shown in Fig. 8a. The statistical uncertainty in the slope of the absorbance increase, and thus in the absorption coefficient, was on the order of a few percent. Plotted in Fig. 8b is the square root of the measured absorption coefficient versus photon energy. The linearity of the data in the figure suggests that the observed absorption in the material behind the shock front was due to an indirect band gap.<sup>39</sup> Extrapolation of the curve to

$\alpha=0$  provides an estimate of  $1.52 \pm 0.03$  eV for the band gap energy. This value is within the range of values (1.5-1.7 eV) reported in the literature for the band gap energy of the high pressure rock salt phase.<sup>33,34</sup>

A total of six experiments were performed on both *a*- and *c*-axis crystals shocked to stresses above 5.9 GPa. Similar results were obtained for all of these experiments, with measured band gaps ranging from 1.49-1.53 eV (similar uncertainties). Further discussion of these results can be found elsewhere;<sup>28,35,40</sup> the results are shown to provide a sense of the measurement precision obtained using the experimental method presented here.

## V. Concluding Remarks

An experimental method was developed to perform picosecond time-resolved electronic spectroscopy in single-event, plate impact, shock wave experiments. This method builds upon previous work used to obtain nanosecond time-resolved measurements.<sup>12,15-18</sup> However, due to the short time duration (12.7 ns) of the picosecond experiments, several issues not relevant in nanosecond resolution experiments become important. The developments presented here to overcome these experimental issues enabled absorption/transmission measurements to be performed in single-event, shock wave experiments with 100 ps time resolution. This experimental capability is expected to be useful in understanding the atomic/molecular mechanisms which govern certain shock-induced processes, such as chemical reactions and phase transitions. Such measurements were used to investigate the initial stages of the shock-induced phase transformation in cadmium sulfide.<sup>28,35,40</sup>

We note that the time resolution of these experiments was limited by the difficulty of synchronization introduced by the effects of non-planar impact. In the triggering scheme described here, the arrival of the shock wave at the probed region could be predicted to within only 2 to 4 ns; this was due to the effects of non-planar impact and the requirement that the trigger pins and the probed region of the sample necessarily be laterally displaced. The effect of non-planar impact on synchronization would need to be eliminated in order to reach higher time resolution in these experiments. Work is currently underway to address this need.

Finally, the developments presented here described a method to incorporate a Nd:YAG laser into a plate-impact, shock wave experiment. Thus, we expect these developments to also be

useful for shock wave experiments involving Raman, fluorescence, or other types of spectroscopy which require the use of a laser.

### **Acknowledgments**

The assistance of Dave Savage with the impact experiments is gratefully acknowledged. The developments reported here were supported by the ONR Grant N000149510311 (Program Manager, Dr. R.S. Miller) under the DURIP initiative.



## REFERENCES

1. *Shock Compression of Condensed Matter--1991*, edited by S.C. Schmidt, R.D. Dick, J.W. Forbes, and D.G. Tasker (Elsevier, Amsterdam, 1992), chapters 9 and 10
2. *High Pressure Science and Technology--1993*, edited by S.C. Schmidt, J.W. Shaner, G.A. Samaria, and M. Ross (AIP Press, New York, 1994), chapters 16 and 17
3. D. Bancroft, E.L. Peterson, and S. Minshall, *J. Appl. Phys.* **27**, 291 (1956)
4. G.E. Duvall and R.A. Graham, *Rev. Mod. Phys.* **49**, 523 (1977)
5. Y.M. Gupta, in *Shock Compression of Condensed Matter--1991*, edited by S.C. Schmidt, R.D. Dick, J.W. Forbes, and D.G. Tasker (Elsevier, Amsterdam, 1992), p. 15
6. R. Cheret, *Detonation of Condensed Explosives* (Springer-Verlag, New York, 1993)
7. F.S. Minshall, in *Response of Metals to High Velocity Deformation*, edited by P.G. Shewmon and W.F. Zackay (Interscience, New York, 1961)
8. R.E. Duff and F.S. Minshall, *Phys. Rev.* **108**, 1207 (1957)
9. R.H. Warnes, *J. Appl. Phys.* **38**, 4629 (1967)
10. A.N. Dremin, S.V. Pershin, and V.F. Pogorelov, *Combust. Explos. Shock Waves* **1**, 1 (1965)
11. G.E. Duvall and G.R. Fowles, in *High Pressure Physics and Chemistry*, edited by R.S. Bradley (Academic, New York, 1963), Vol. II
12. Y.A. Gruzdkov and Y.M. Gupta, *J. Phys. Chem. A* **102**, 2322 (1998)
13. Y.A. Gruzdkov and Y.M. Gupta, *J. Phys. Chem. A*, to be published
14. D.B. Hayes, *Experimental Determination of Phase Transition Rates in Shocked Potassium Chloride*, Ph.D. Thesis, Washington State University, 1973 (unpublished); D.B. Hayes, *J. Appl. Phys.* **45**, 1208 (1974)
15. C.S. Yoo, Y.M. Gupta, and G.E. Duvall, in *Shock Compression of Condensed Matter--1989*, edited by S.C. Schmidt, J.N. Johnson, and L.W. Davison (Elsevier, Amsterdam, 1990); C.S. Yoo and Y.M. Gupta, *J. Phys. Chem.* **94**, 2857 (1990); C.S. Yoo and Y.M. Gupta, *J. Phys. Chem.* **96**, 7555 (1992)
16. Y.M. Gupta, *High Pressure Research* **10**, 717 (1992)
17. C.P. Constantinou, J.M. Winey, and Y.M. Gupta, *J. Phys. Chem.* **98**, 7767 (1994)
18. J.M. Winey and Y.M. Gupta, *J. Phys. Chem. A* **101**, 9333 (1997)

19. R.L. Gustavsen and Y.M. Gupta, J. Appl. Phys. **69**, 918 (1991); R.L. Gustavsen and Y.M. Gupta, J. Chem. Phys. **95**, 451 (1991)
20. C.S. Yoo, Y.M. Gupta, and P.D. Horn, Chem. Phys. Lett. **159**, 178 (1989)
21. Y.M. Gupta, P.D. Horn, and C.S. Yoo, Appl. Phys. Lett. **55**, 33 (1989)
22. R.L. Gustavsen and Y.M. Gupta, J. Appl. Phys. **75**, 2837 (1994)
23. G.I. Pangilinan and Y.M. Gupta, J. Phys. Chem. **98**, 4522 (1994)
24. J.M. Winey and Y.M. Gupta, J. Phys. Chem. B **101**, 10733 (1997)
25. Y.M. Gupta, D.D. Kough, D.F. Walker, K.C. Dao, D. Henley, and A. Urweider, Rev. Sci. Instrum. **51**, 183 (1980)
26. To ensure that the surface of the pins were parallel to the shock front, the following procedure was performed. First, the pins were mounted in an aluminum ring (this ring would also serve as a sample holder in the target assembly). The ring was then lapped until the copper plating was removed from all three pin surfaces. This ensured that the pins were all in the same plane, and that the pin surfaces were all parallel to the front surface of the mount, and thus the front buffer window. The pin surfaces were then replated with copper using a vacuum deposition system.
27. Operation and Maintenance Manual for the Powerlite 8000 Series Laser, Continuum, 3150 Central Expressway, Santa Clara, CA, 1993 (unpublished)
28. M.D. Knudson, *Picosecond Electronic Spectroscopy to Understand the Shock-Induced Phase Transition in Cadmium Sulfide*, Ph.D. Thesis, Washington State University, 1998 (unpublished)
29. Details concerning the logic circuit can be obtained from the authors; direct all inquiries to K.A. Zimmerman
30. S.L. Wymer Meardon, *The Elements of Fiber Optics* (Prentice-Hall, Inc., New Jersey, 1993) p. 38
31. *American Institute of Physics Handbook, 3rd edition*, edited by D.E. Gray (McGraw-Hill Book Co., New York, 1972) p. 6-28
32. *Numerical Data and Functional Relationships in Science and Technology, New Series, Group III, Vols 17a and 22a*, edited by K.H. Hellwege and O. Madelung (Springer, Berlin, 1982)

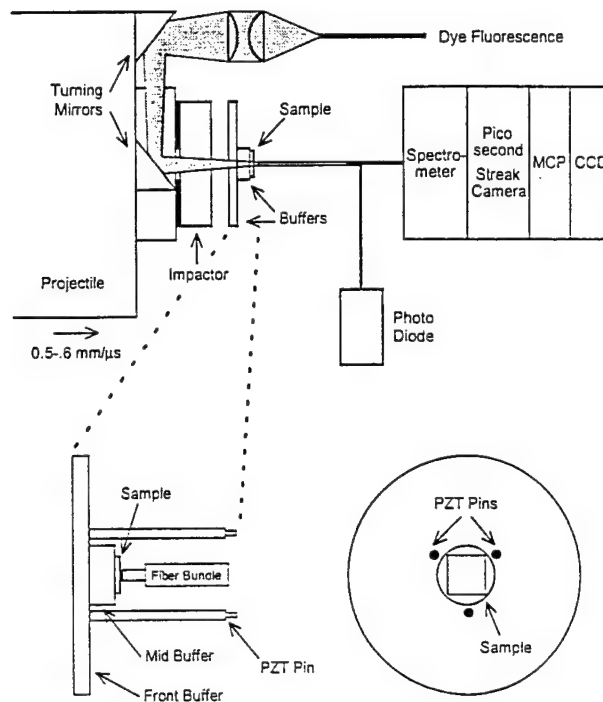


Fig. 1. The experimental configuration used to obtain picosecond time-resolved absorption/transmission measurements in plate impact, shock wave experiments. Also shown is an enlargement of the sample assembly, displaying the concentric arrangement of the PZT trigger pins about the probed region of the sample.

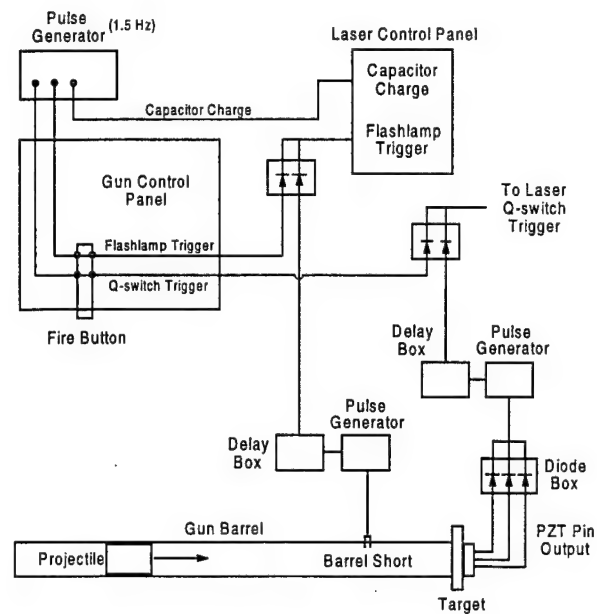


Fig. 2. Schematic view of the electrical configuration used to incorporate the Nd:YAG laser into the plate-impact experiment.

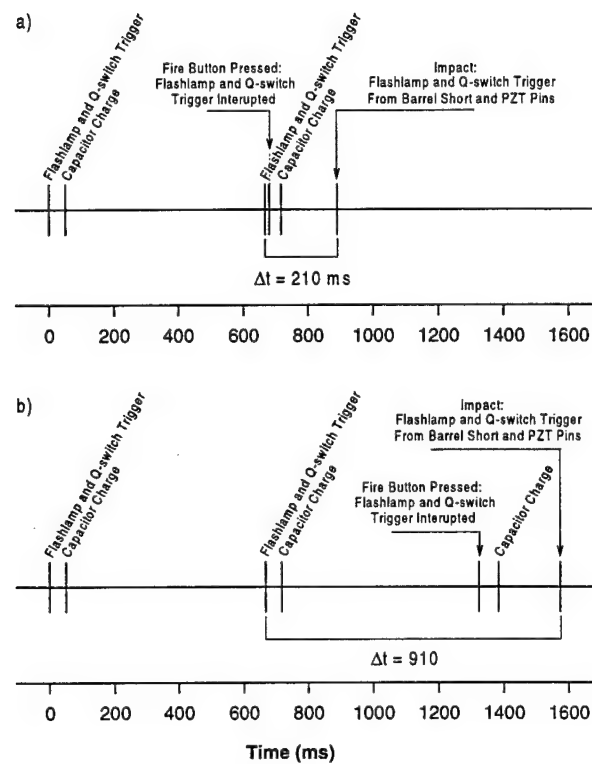


Fig. 3. Timelines showing the (a) minimum and (b) maximum time interval between the laser pulse obtained during the shock experiment and the pulse immediately prior to that pulse when synchronizing the Nd:YAG laser to the gas gun.

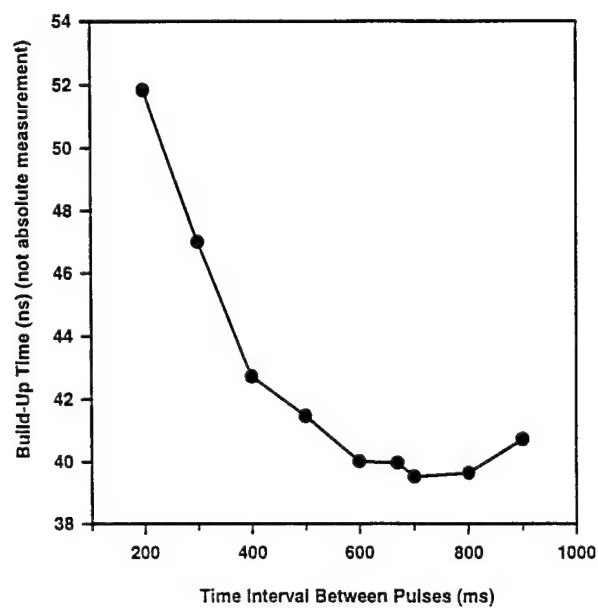


Fig. 4. Build-up time of the Nd:YAG as a function of time interval between the pulse obtained during the shock experiment and the pulse immediately prior to that pulse. The data is taken in reference to the laser running at a repetition rate of 1.5 Hz, i.e. regular time interval of 667 ms.

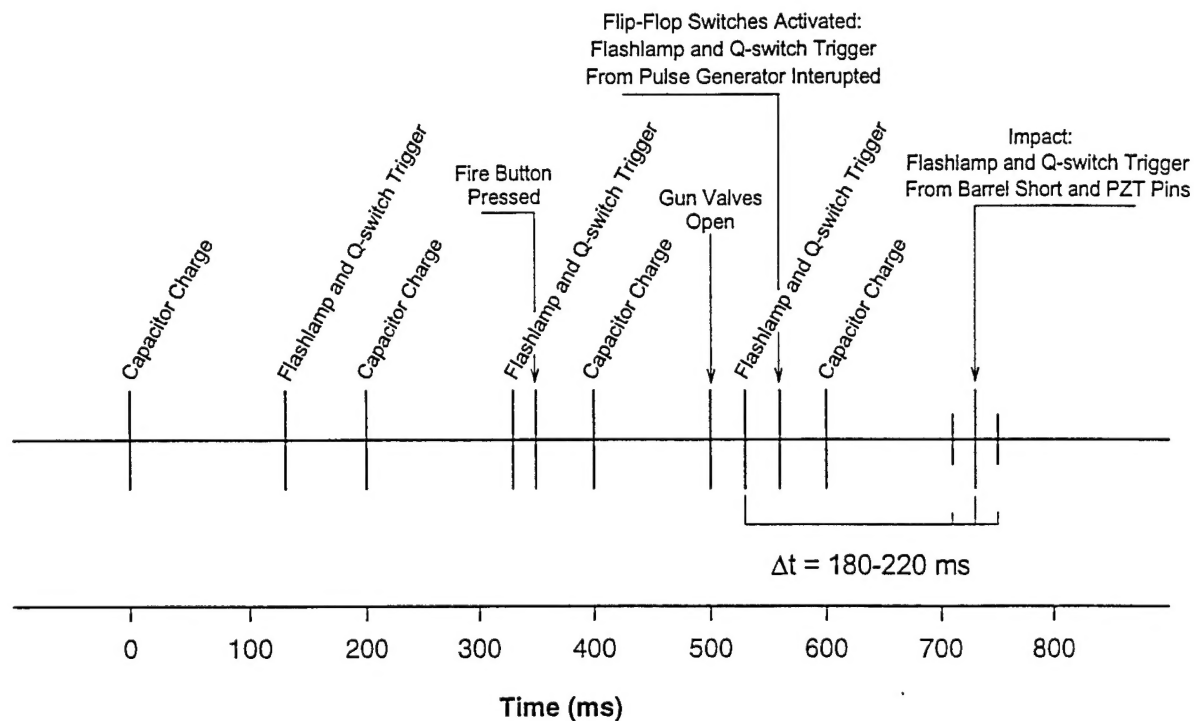


Fig. 5. Timeline showing the time interval between the laser pulse obtained during the shock experiment and the pulse immediately prior to that pulse when synchronizing the gas gun to the Nd:YAG laser.



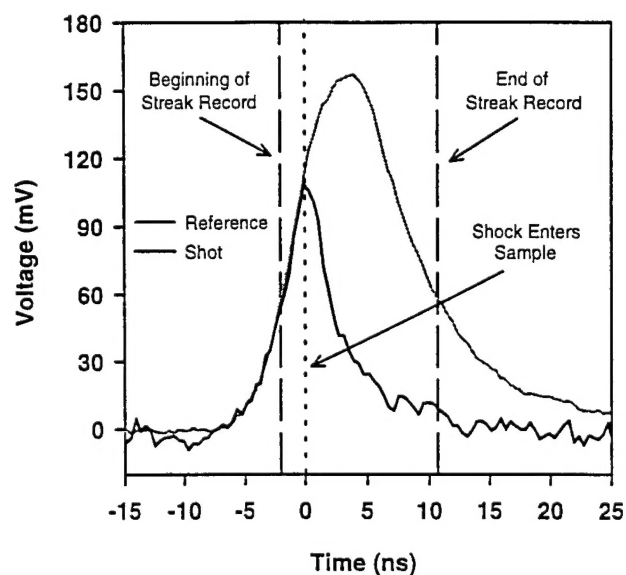


Fig. 6. Typical experimental result obtained from the fast photodiode, showing the integrated intensity of transmitted light through the sample. This particular experiment was performed on CdS shocked to 8.8 GPa along the crystal *c*-axis. The reproducibility of the reference pulse is on the order of 5%.

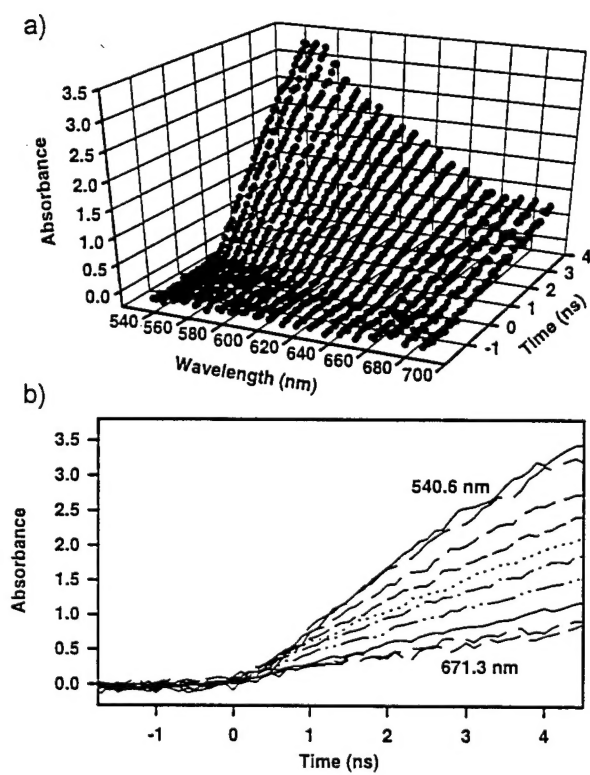


Fig. 7. Typical experimental results obtained from the picosecond detection system. This result corresponds to an experiment performed on CdS shocked to 8.8 GPa along the crystal *c*-axis.

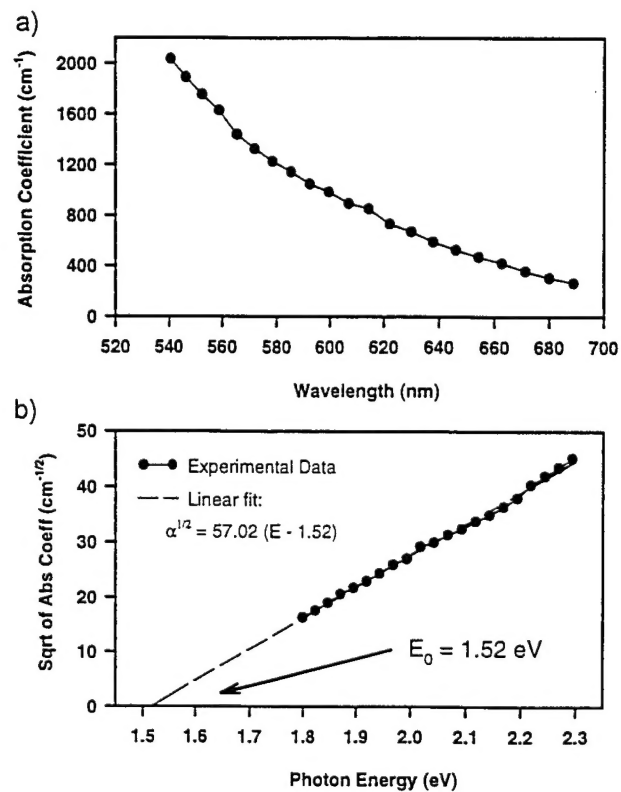


Fig. 8. Absorption coefficient as a function of wavelength and photon energy for an experiment on *c*-axis CdS shocked to 8.8 GPa.